








Article

Green Synthesis and Antimicrobial Activities of Silver Nanoparticles Using *Calotropis gigantea* from Ie Seu-Um Geothermal Area, Aceh Province, Indonesia

Pati Kemala ^{1,2}, Rinaldi Idroes ^{1,2,3,4,*} , Khairan Khairan ^{2,3,4}, Muliadi Ramli ² , Zulkarnain Jalil ⁵ , Ghazi Mauer Idroes ⁶, Trina Ekawati Tallei ⁷ , Zuchra Helwani ⁸ , Eka Safitri ² , Muhammad Iqhrammullah ⁹  and Rosnani Nasution ²

- ¹ Graduate School of Mathematics and Applied Sciences, Universitas Syiah Kuala, Banda Aceh 23111, Indonesia
² Department of Chemistry, Faculty of Mathematics and Natural Sciences, Universitas Syiah Kuala, Banda Aceh 23111, Indonesia
³ Department of Pharmacy, Faculty of Mathematics and Natural Sciences, Universitas Syiah Kuala, Banda Aceh 23111, Indonesia
⁴ Herbal Medicine Research Center, Universitas Syiah Kuala, Banda Aceh 23111, Indonesia
⁵ Department of Physics, Faculty of Mathematics and Natural Sciences, Universitas Syiah Kuala, Banda Aceh 23111, Indonesia
⁶ Department of Chemical Engineering, Faculty of Engineering, Universitas Syiah Kuala, Banda Aceh 23111, Indonesia
⁷ Department of Biology, Faculty of Mathematics and Natural Sciences, Sam Ratulangi University, Manado 95115, Indonesia
⁸ Department of Chemical Engineering, Faculty of Engineering, Universitas Riau, Pekanbaru 28293, Indonesia
⁹ Department of Life Sciences and Chemistry, Jacobs University Bremen, Campus Ring 1, 28759 Bremen, Germany
* Correspondence: rinaldi.idroes@unsyiah.ac.id



Citation: Kemala, P.; Idroes, R.; Khairan, K.; Ramli, M.; Jalil, Z.; Idroes, G.M.; Tallei, T.E.; Helwani, Z.; Safitri, E.; Iqhrammullah, M.; et al. Green Synthesis and Antimicrobial Activities of Silver Nanoparticles Using *Calotropis gigantea* from Ie Seu-Um Geothermal Area, Aceh Province, Indonesia. *Molecules* **2022**, *27*, 5310. <https://doi.org/10.3390/molecules27165310>

Academic Editor: Artur M. S. Silva

Received: 27 July 2022

Accepted: 16 August 2022

Published: 20 August 2022

Publisher's Note: MDPI stays neutral with regard to jurisdictional claims in published maps and institutional affiliations.



Copyright: © 2022 by the authors. Licensee MDPI, Basel, Switzerland. This article is an open access article distributed under the terms and conditions of the Creative Commons Attribution (CC BY) license (<https://creativecommons.org/licenses/by/4.0/>).

Abstract: Herein, we report our success synthesizing silver nanoparticles (AgNPs) using aqueous extracts from the leaves and flowers of *Calotropis gigantea* growing in the geothermal manifestation Ie Seu-Um, Aceh Besar, Indonesia. *C. gigantea* aqueous extract can be used as a bio-reductant for $\text{Ag}^+ \rightarrow \text{Ag}^0$ conversion, obtained by 48h incubation of Ag^+ , and the extract mixture in a dark condition. UV-Vis characterization showed that the surface plasmon resonance (SPR) peaks of AgNPs-leaf *C. gigantea* (AgNPs-LCg) and AgNPs-flower *C. gigantea* (AgNPs-FCg) appeared in the wavelength range of 410–460 nm. Scanning electron microscopy energy-dispersive X-ray spectrometry (SEM-EDS) revealed the agglomeration and spherical shapes of AgNPs-LCg and AgNPs-FCg with diameters ranging from 87.85 to 256.7 nm. Zeta potentials were observed in the range of -41.8 to -25.1 mV. The Kirby-Bauer disc diffusion assay revealed AgNPs-FCg as the most potent antimicrobial agent with inhibition zones of 12.05 ± 0.58 , 11.29 ± 0.45 , and 9.02 ± 0.10 mm for *Escherichia coli*, *Staphylococcus aureus*, and *Candida albicans*, respectively. In conclusion, aqueous extract from the leaves or flowers of *Calotropis gigantea* may be used in the green synthesis of AgNPs with broad-spectrum antimicrobial activities.

Keywords: silver nanoparticles; geothermal manifestation; Ie Seu-Um; *C. gigantea*; antimicrobial activities

1. Introduction

Researchers have long studied plant extracts for their broad spectrum of medicinal properties such as anti-inflammatory [1], antibacterial [2,3], antifertility [4], termiticide, and nematocide activities [5]. Studies on plant extracts have recently gained more interest during the COVID-19 pandemic in the effort to find efficacious antiviral agents [6–9]. Notably, the bioactive compounds contained in plant extracts are strongly influenced by environmental factors [10]. For example, more diverse metabolites and higher-yield extracts

were produced by plants that grow in coastlines and geothermal areas compared with those in other areas [11].

Several areas in Aceh Province have geothermal potential stemming from volcanic activities, including Mount Seulawah Agam, located in the Aceh Besar District [12,13]. Mount Seulawah Agam is a potential site for the construction of a geothermal power plant with an estimated energy capacity of 230 MW [14]. This mountain has several manifestations, namely Ie Brouk [15], Ie Seu-Um [16], and Ie Jue [17]. Bursts of mineral-rich water in each of these manifestations have spread to the surrounding environment, contributing to the mineral disposition in the soil, which subsequently affects the biosynthesis of plants therein. One of the plants thriving in the geothermal environment is *Calotropis gigantea*, which intensely grows in the area.

In a previous investigation, the ethanolic extract from the leaves of *C. gigantea* (collected from the manifestation of Ie Jue) was observed to have effective antibacterial activities against Gram-negative (*Porphyromonas gingivalis*) and Gram-positive bacteria (*Solobacterium moorei*) [18]. Another study witnessed that the lignan glycoside compounds contained in the latex of *C. gigantea* from the manifestation of Ie Brouk contained potential antiviral properties against influenza virus and anti-SARS-CoV-2 in silico [19]. Of the three aforementioned geothermal manifestations in Mount Seulawah Agam, *C. gigantea* is abundant in the Ie Seu-Um manifestation [20].

In a recent review, silver nanoparticles (AgNPs) were highlighted to possess strong antibacterial properties against Gram-negative and -positive bacteria, including the strains that have developed multidrug-resistant mechanisms [21]. Other than the common mechanism of the disintegrating bacterial cell wall membrane, AgNPs are uniquely capable of causing bacterial DNA and protein dysfunction by interacting with phosphorous or sulfur groups [22–24]. AgNPs may also induce apoptosis against bacterial cells by producing reactive oxygen species and free radicals, concomitant with the release of Ag^+ from AgNPs and followed by a reaction with thiol groups [22–24]. Therefore, it is of importance to develop AgNPs as an efficacious antibacterial agent to curb the global health burden caused by bacterial infection, especially with the increasing trend of multidrug-resistant bacteria [25]. To achieve that, green synthesis using bioactive phytochemicals may enhance the bioactivity of AgNPs, as they possess the ability to overcome bacterial-drug-resistant mechanisms [21,26]. Green nanoparticle synthesis is defined as a means of obtaining metal nanoparticles with the help of bioreductor, plant, fungal, or bacterial extracts (produced using a green solvent, such as water). Due to the exclusion of toxic and ecotoxic reagents from the procedure, green synthesis is eco-friendly by nature and safe.

Herein, we used flower and leaf extracts from *C. gigantea* collected from the Ie Seu-Um geothermal manifestation to green synthesize AgNPs. Antimicrobial activities in *S. aureus*, *E. coli*, and *C. albicans* were tested to evaluate the bioactivity of the synthesized AgNPs. Multiple reports have been published regarding the green synthesis of silver nanoparticles [27,28]. However, research highlighting geothermal plants is currently underreported, hence the novelty of our research. Moreover, we conducted a longitudinal comparison between the extracts yielded from the flower and those from the leaf of *C. gigantea*; the results provide significant implications for the development of green nanoparticle synthesis research.

2. Results and Discussion

2.1. Green Synthesis AgNPs-LCg and AgNPs-FCg

The AgNPs produced from the leaves and flowers of *C. gigantea* were labeled as AgNPs-LCg and AgNPs-FCg, respectively. Color changing occurred and acted as an indicator of the $\text{Ag}^+ \rightarrow \text{Ag}^0$ reaction (Figure 1). In a mixture producing AgNPs-LCg, the transparent and yellowish solution turned into a blackish-brown solution following the incubation process. In the case of AgNPs-FCg, the colorless solution transformed into a yellow-brown solution (Figure 1). Similarly, previous reports have shown the color

changing into yellow-brown [29–32] or dark brown [33–38] following the green synthesis of AgNPs.

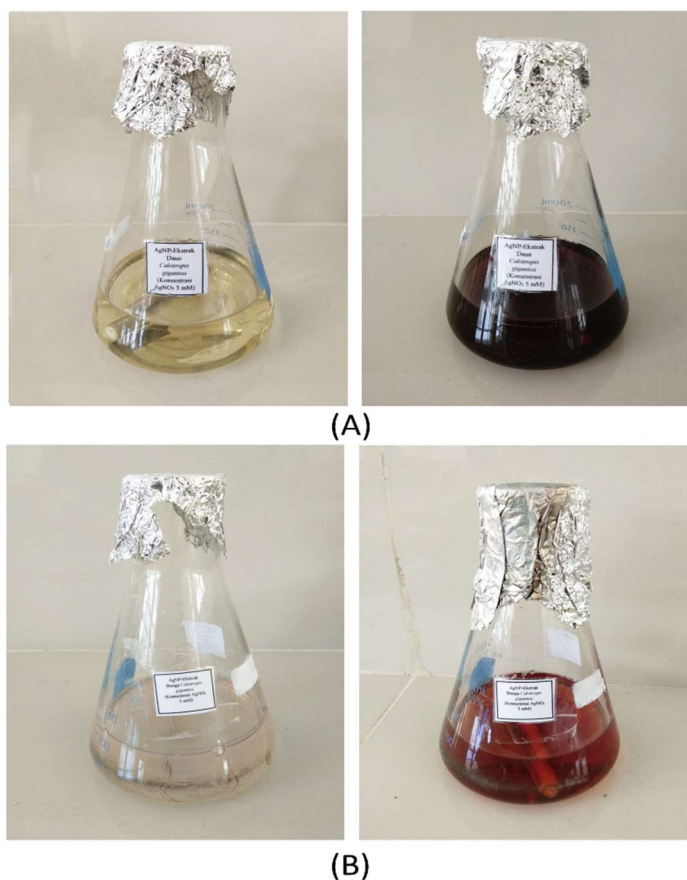


Figure 1. Visual appearance of AgNO₃ solution mixed with leaves (A) and flower extract (B) from geothermal *C. gigantea* before (left) and after (right) the dark incubation.

The difference in color transformation between AgNPs-LCg and AgNPs-FCg could be attributed to the phytometabolite components contained in the leaves or flowers of the geothermal *C. gigantea*. Thus, we proceeded with our investigation on qualitative phytochemical screening, for which the data are presented in Table 1. Both extracts were positive for containing alkaloids, saponins, phenolics, and tannins. Flavonoids and terpenoids were detected in the flower extract but not in the leaf extract. Meanwhile, steroids were only observable in the leaf extract.

Table 1. Qualitative phytochemical analysis of AgNPs-FCg and AgNPs-LCg.

| Secondary Metabolites | AgNPs-FCg | AgNPs-LCg |
|-----------------------|-----------|-----------|
| Saponins | +(ve) | +(ve) |
| Phenolic | +(ve) | +(ve) |
| Tannins | +(ve) | +(ve) |
| Flavonoids | +(ve) | –(ve) |
| Terpenoids | +(ve) | –(ve) |
| Steroids | –(ve) | +(ve) |
| Alkaloids | +(ve) | +(ve) |

Note: +(ve): positive; –(ve): negative.

2.2. Characterization of Silver Nanoparticles (AgNPs-LCg and AgNPs-FCg)

2.2.1. UV-Vis Spectrophotometry Analysis

UV-Vis spectrophotometers are rapid, easy-to-use, and sensitive tools frequently used for initial characterization of metal nanoparticles synthesized using biological methods [39]. The chromophore of secondary metabolites present in metal-reducing organic compounds could perform light absorption in UV and UV-Vis wavelength ranges [39]. Phytometabolites may act as electron donors and mediate the reduction of silver ions [33], thereby initiating surface plasmon resonance (SPR). This phenomenon is a complicated process defined as the excitation and coherent oscillation of electrons in an incoming electromagnetic field [39]. The absorption peak profile is dependent on the functional group and chromoionophore compositions of the plant extract and the extract concentration used in the AgNP synthesis [33].

The SPR peaks of the AgNPs-FCg samples prepared using AgNO₃ with concentrations of 2, 5, and 9 mM were found at 440, 450, and 460 nm, respectively (Figure 2). Meanwhile, the SPR of the AgNPs-LCg samples synthesized using AgNO₃ with 2, 5, and 9 mM were found at 440, 430, and 460 nm, respectively (Figure 2). Our results do not deviate much in comparison with those previously reported [34,40]. As a comparison, a study preparing AgNPs using Indian *C. gigantea* flower reported an SPR peak at 422 nm [34]. In another study, UV-Vis characterization on AgNPs produced from *C. gigantea* leaf extract collected in the Shudqum region, Saudi Arabia, revealed an SPR peak at 450 nm [40].

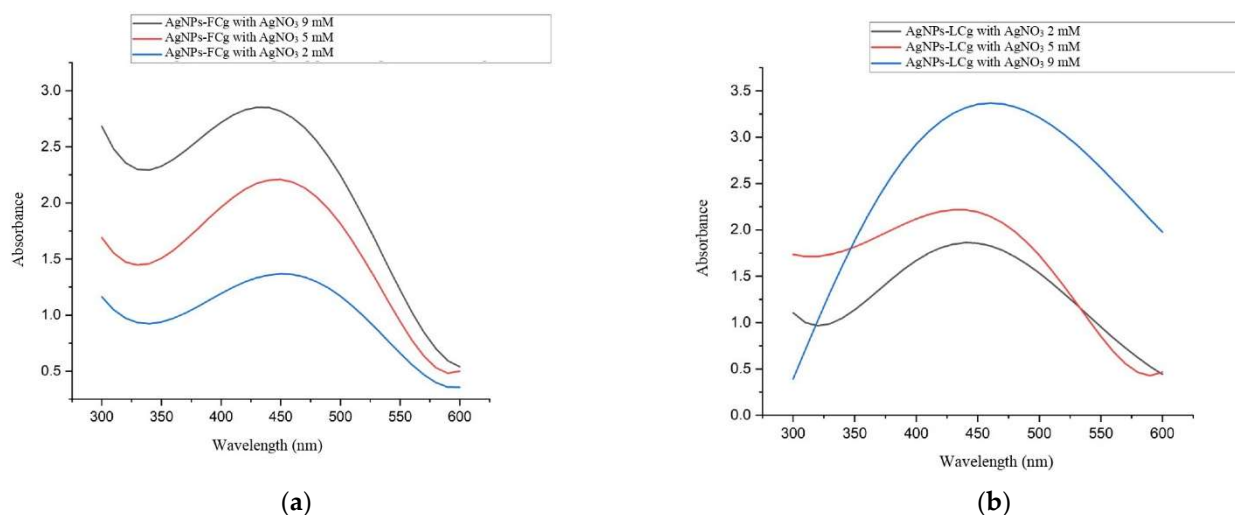


Figure 2. UV-Vis spectrophotometry characterization of (a) AgNPs-FCg and (b) AgNPs-LCg.

2.2.2. Fourier Transform Infrared (FTIR) Analysis

We used Fourier transform infrared (FTIR) characterization to identify functional groups suspected to be involved in the AgNPs synthesis, for which the data are presented in Figure 3. The spectral profiles of both AgNPs-FCg and AgNPs-LCg suggest the presence of O—H stretching, C=C stretching, N—H bending, and C—H bending vibrations assigned for the absorbance peaks observed at 3250, 2100, 1600, and 610 cm⁻¹, respectively. A previous report suggested the involvement of the N—H functional group in AgNPs synthesis [41]. The absorption of O—H showed that polar compounds (likely flavonoids or phenolics) from plants (Table 1) are involved in the green synthesis of AgNPs. It was also claimed that the O—H and amine groups are components that function as capping agents to stabilize silver nanoparticles [42]. Our findings agree with previously reported AgNPs-LCg results showing that the presence of groups at 3421 and 2923 cm⁻¹ are assigned to the bending vibration of N—H, 2853 cm⁻¹ is assigned to the stretching vibration of C—H in alkanes, 2361 cm⁻¹ indicates a primary amine group, 1457 cm⁻¹ is assigned to the stretching vibration of protein, and 1116 cm⁻¹ is assigned to the stretching vibration of C—O [40].

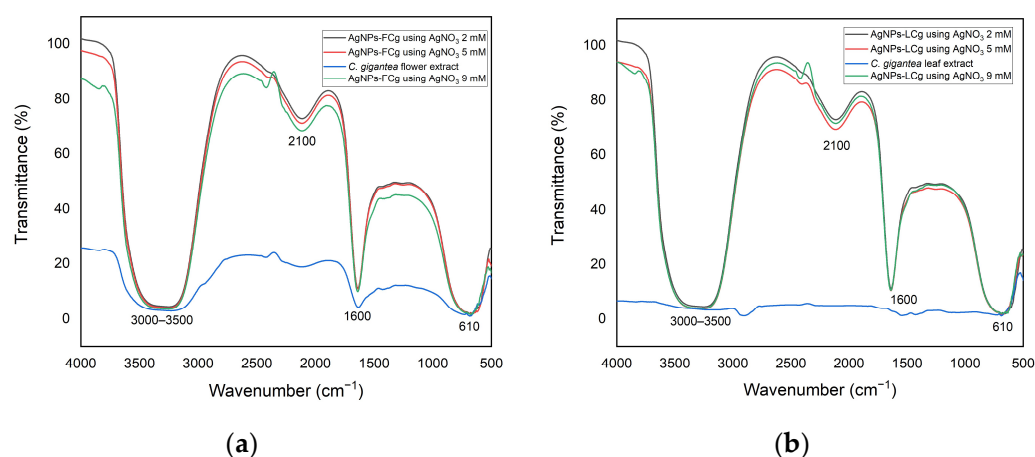


Figure 3. FTIR spectra of (a) AgNPs-FCg and (b) AgNPs-LCg at several concentrations of AgNO₃.

2.2.3. SEM-EDS Analysis

The scanning electron microscopy energy-dispersive X-ray spectroscopy (SEM-EDS) images of AgNPs-FCg and AgNPs-LCg surfaces are presented in Figure 4a,b, respectively. The formed AgNPs-FCg and AgNPs-LCg were observed to be agglomerated. In general, the morphology of formed AgNPs-FCg and AgNPs-LCg is spherical. The agglomeration of AgNPs synthesized from plants has been previously reported by those using the leaves of *C. gigantea* [40], *Andrographis paniculata*, *Phyllanthus niruri*, *Tinuspora cordifolia* [29], *Nigella sativa* [43], *Brilliantaisia patula*, *Crossopteryx febrifuga*, *Senna siamea* [44], *Lampranthus coccineus*, *Malephora lutea* [35], *Platycodon grandiflorum* [30], *Memecylon umbellatum* Burm F [45], and *Malva parviflora* [33]. The EDS spectra of AgNPs-FCg and AgNPs-LCg, indicating the elements present in each sample, are presented in Figure 5. The list of elements of each sample obtained from the EDS analysis is provided in Figure 5. According to the results of the EDS analysis, metallic silver predominated among the elements observed in the sample. Therefore, this analysis confirmed that the produced particles were silver nanoparticles (AgNPs). Other elements are thought to be derived from secondary metabolites found in the *C. gigantea* plant that grows in mineral-rich geothermal areas.

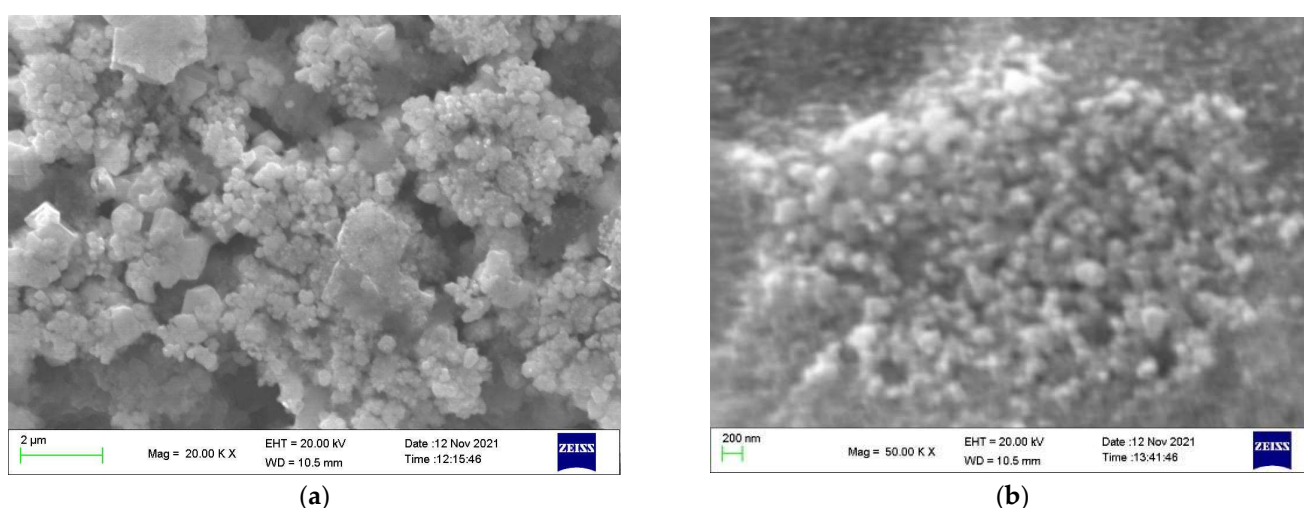


Figure 4. SEM image of AgNPs-LCg (a) and AgNPs-FCg (b) displayed at 20,000 \times and 50,000 \times magnification, respectively.

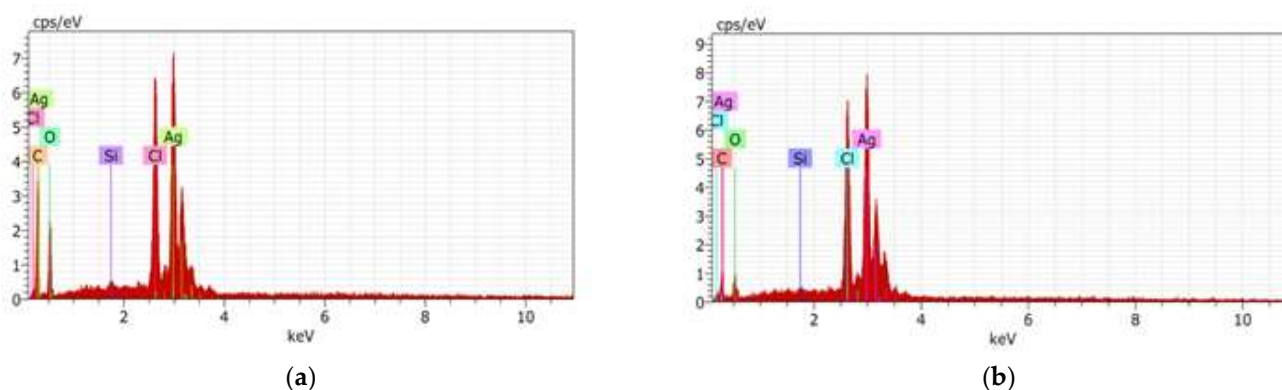


Figure 5. EDS spectra of (a) AgNPs-FCg and (b) AgNPs-LCg at several concentrations of AgNO₃.

2.2.4. Zeta Potential Analysis

The results of the zeta potential analysis on AgNPs-LCg and AgNPs-FCg produced from the various concentrations of AgNO₃ (2, 5, and 9 mM) are presented in Table 2. The synthesized AgNPs-LCg and AgNPs-FCg were relatively stable at -25.1 to -41.8 mV, respectively. Generally, the larger the negative zeta potential value, the more stable the AgNPs formed [30,46]. In this study, the concentration of AgNO₃ as a metal precursor solution affected the stability of the produced AgNPs. In AgNPs-FCg, the stability increased as the concentration of AgNO₃ increased. For AgNPs-LCg, the highest stability value was obtained when the AgNO₃ concentration was 5 mM.

Table 2. Zeta potential analysis parameters of AgNPs-LCg and AgNPs-FCg.

| [AgNO ₃] | AgNPs-FCg (Mean ± SD) | | AgNPs-LCg (Mean ± SD) | |
|----------------------|-----------------------|------------------|-----------------------|-------------------|
| | Stability (mV) | Size (nm) | Stability (mV) | Size (nm) |
| 2 mM | -33.05 ± 0.00 | 256.7 ± 2.82 | -40.5 ± 0.56 | 227.65 ± 0.07 |
| 5 mM | -30.3 ± 0.00 | 200.8 ± 0.14 | -41.8 ± 0.14 | 87.85 ± 0.91 |
| 9 mM | -25.1 ± 0.00 | 163.5 ± 1.06 | -31.35 ± 0.7 | 188.35 ± 3.32 |

The sizes of AgNPs-LCg and AgNPs-FCg obtained widely ranged: 163.5 ± 1.06 – 256.7 ± 2.82 and 87.85 ± 0.91 – 227.65 ± 0.07 , respectively. The smallest size of the AgNPs was the AgNPs-LCg obtained when the [AgNO₃] was 5 mM. The AgNPs size correlated with the SPR peak measured by UV–Vis spectroscopy, where the lower the SPR wavelength, the smaller the particle size obtained [47]. Therefore, in this present study, the particle size obtained through zeta potential analysis is corroborated by the earlier finding from UV–Vis spectroscopy, where the AgNPs-LCg produced from AgNO₃ 5 mM had the lowest SPR wavelength.

2.3. Antimicrobial Activity of Silver Nanoparticles (AgNPs-LCg and AgNPs-FCg)

One of the properties of AgNP that has long been a hot topic is its antimicrobial activity [34,48]. AgNP has attracted the interest of researchers because it has antibacterial, antifungal, antiviral, antiangiogenic, and cytotoxic properties against cancer cells that have not been replaced by the properties of other metals [39]. The exact mechanism by which AgNPs have toxic or antimicrobial activity remains a mystery and is a topic of debate [34]. Several studies have shown that the spherical shape, concentration, and type of silver nanoparticles may play a key role in the inhibition of bacteria, which are absorbed in bacterial cells to interact with bacterial DNA and proteins causing their damage, further resulting in more oxidative stress through the generation of reactive oxygen species (ROS). ROS accumulate into the mitochondrial membrane of bacteria, resulting in dysfunctional mitochondria, thereby inhibiting bacterial growth [49].

In this study, antibacterial and antifungal evaluations of AgNPs-LCg and AgNPs-FCg were carried out using two bacterial pathogens (*E. coli* and *S. aureus*, which represented Gram-negative and -positive bacteria, respectively) and one fungal pathogen (*C. albicans*). Images of the inhibition of the foregoing pathogens performed by AgNPs-LCg and AgNPs-FCg on Kirby-Bauer disc diffusion assays are presented in Figure 6. Based on the results obtained, the samples of AgNPs-LCg and AgNPs-FCg were found to inhibit the growth of bacteria and fungi as the inhibitory properties of bacterial and fungal pathogens increased in proportion to the increase in AgNO₃ concentration in the synthesis process. The quantitative data of the inhibition zones are presented in more detail in Table 3. AgNPs-FCg had the highest antimicrobial activity in *S. aureus*, which was 12.05 ± 0.58 mm, followed by *E. coli* at 11.29 ± 0.45 mm and *C. albicans* at 9.02 ± 0.10 mm. Meanwhile, AgNPs-LCg had the highest antimicrobial activity in *S. aureus*, which was 10.60 ± 0.22 mm, followed by *C. albicans* at 8.90 ± 0.25 mm and *E. coli* at 8.40 ± 0.33 mm.

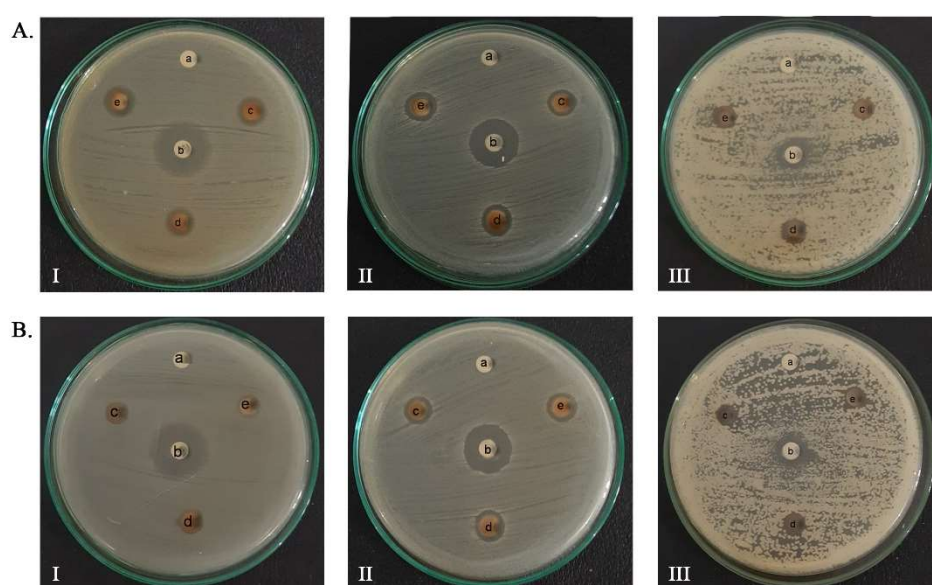


Figure 6. Antimicrobial activity analysis: (A) AgNPs-FCg; (B) AgNPs-LCg (I: *E. coli* bacteria, II: *S. aureus* bacteria, III: *C. albicans* fungus where a: negative control, b: positive control, c: sample with AgNO₃ concentration of 2 mM, d: sample with AgNO₃ concentration 5 mM, e: sample with 9 mM AgNO₃ concentration).

Table 3. Antimicrobial activities of AgNPs-FCg and AgNPs-LCg.

| Sample | Concentration of [AgNO ₃] (mM) | Inhibition Zone, Mean \pm SD (mm) | | |
|-----------|--|-------------------------------------|-------------------------|-------------------------|
| | | <i>Staphylococcus aureus</i> | <i>Escherichia coli</i> | <i>Candida albicans</i> |
| AgNPs-FCg | 2 | 10.53 ± 0.57 | 9.89 ± 0.56 | 7.52 ± 0.11 |
| | 5 | 11.24 ± 0.83 | 10.54 ± 0.59 | 8.12 ± 0.16 |
| | 9 | 12.05 ± 0.58 | 11.29 ± 0.45 | 9.02 ± 0.10 |
| AgNPs-LCg | 2 | 10.10 ± 0.08 | 7.85 ± 0.18 | 7.37 ± 0.29 |
| | 5 | 10.48 ± 0.23 | 8.18 ± 0.13 | 7.95 ± 0.26 |
| | 9 | 10.60 ± 0.22 | 8.40 ± 0.33 | 8.90 ± 0.25 |
| Control | | 17.74 ± 0.28^a | 19.45 ± 0.69^b | 10.20 ± 0.12^c |

Control: ^a vancomycin; ^b gentamicin; ^c ketoconazole.

The antibacterial activity of *S. aureus* was significantly different between the AgNPs-LCg and AgNPs-FCg inhibition zones. The AgNPs-LCg inhibition zone with 9 mM AgNO₃ (which was the highest concentration in this study) was almost equivalent to the AgNPs-FCg inhibition zone with 2 mM AgNO₃ (the lowest concentration in this study). In the *E. coli* antibacterial activity test, the AgNPs-LCg inhibition zone with AgNO₃ 9 mM was

lower than the AgNPs-FCg inhibition zone with AgNO₃ 2 mM. This indicates that AgNPs-FCg is more potent in inhibiting the growth of Gram-positive and -negative bacteria than AgNPs-LCg isolated from the Ie Seu-um geothermal area.

The difference in activity between AgNPs-LCg and AgNPs-FCg is thought to be due to differences in secondary metabolite components between the leaves and flowers (please revisit Table 1). The flower extract contained flavonoids, whereas the leaf extract did not. There are at least two possibilities for explaining this finding. Firstly, flavonoids in the flower extract facilitate the higher conversion of Ag⁺ into Ag⁰, attributed to their low redox potentials ranging from 0.23 to 0.75 V (while that of Ag is 0.80 V) [50]. Secondly, flavonoids are likely to bind with the Ag⁰ as a capping agent via a complex formation, as the compounds possess chelating moiety catechol [51]. Members of flavonoids were proven to inhibit bacterial growth by disrupting the cell wall membrane [52]. Therefore, as flavonoids bind to the AgNPs, synergistic inhibitory activities are expected.

It is also noteworthy that in our previous study, the methanol extract of the leaves and stems of *C. gigantea* growing in the Ie Seu-um area was reported to have no inhibition zone on the fungus *C. albicans* [20], but in this study, the antifungal activities against *C. albicans* by AgNPs-LCg and AgNPs-FCg samples were relatively high. With the minimum concentration of AgNO₃ used (2 mM), AgNPs-FCg and AgNPs-LCg were able to inhibit the growth of this fungus by 7.52 ± 0.11 and 7.37 ± 0.29 mm, respectively. AgNO₃ was reported to have the minimum inhibition against the foregoing microbes [53]. Taken altogether, the AgNPs significantly contributed to the antimicrobial activities of our samples. However, as a limitation of this present study, we did not conduct a direct comparison between the prepared AgNPs samples with the extracts and the AgNO₃. Moreover, we did not use commercial AgNPs as a comparison.

3. Materials and Methods

3.1. Materials and Bioindicators

The samples used included the leaves and flowers of *C. gigantea* (Figure 7a) growing in the geothermal manifestation Ie Seu-Um, Aceh Besar, Aceh Province, Indonesia. The sampling locations was 5°32'50.97" N, 95°32'55.10" E at an altitude of 97 m above sea level (Figure 7b).

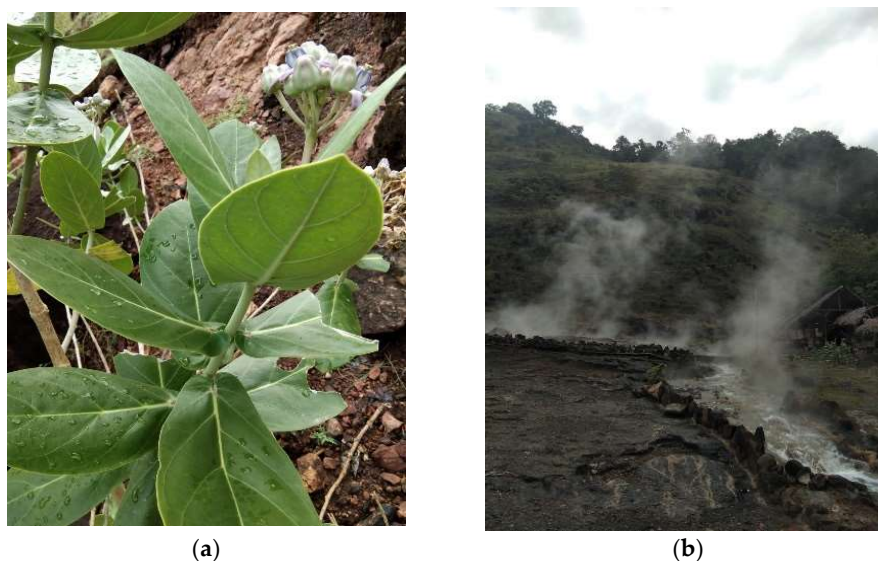


Figure 7. (a) *C. gigantea* plant; and (b) Ie Seu-Um geothermal manifestation area.

The materials used in this study were AgNO₃; Mayer's, Dragendorff, Wagner, and Liberman-Burchard reagents; FeCl₃; Mg powder; gelatin; sulfuric acid; Mueller Hinton agar (MHA) media; and Sabarouds dextrose agar (SDA) purchased from Sigma Aldrich (St. Louis, MO, USA). Other materials used were distilled water, gentamicin, vancomycin,

and ketoconazole. Meanwhile, the bacteria used as bioindicators in this study were *S. aureus* (ATCC 25923) and *E. coli* (ATCC 25922). The fungus used as a bioindicator was *C. albicans* (ATCC 10231).

3.2. Plant Extraction

C. gigantea plants were taken and the flowers and leaves separated, then washed and cut into pieces before drying for two days. Sample extraction was carried out in different ways for both the flowers and leaves. The *C. gigantea* leaf extraction process was carried out by boiling 10 g of leaf sample in 100 mL of distilled water for 20 min and filtered using filter paper [40]. The *C. gigantea* flower was extracted by adding 200 mL of distilled water while stirring at room temperature for 15 min and filtering [34].

3.3. Phytochemical Test

Phytochemical analysis was carried out to examine the contents of alkaloids, saponins, phenolics, tannins, flavonoids, steroids, and terpenoids in the flower and leaf extracts of *C. gigantea*. Phytochemical screening followed the standard method [54]. The alkaloid test used Mayer, Dragendorff, and Wagner reagents. The saponin test was carried out by examining the stable foam after being shaken using distilled water. The steroid test and terpenoid test used Liberman-Burchard reagent. The phenolic test used FeCl_3 and flavonoid test Mg powder. As for the tannin test, gelatin and sulfuric acid were used.

3.4. Green Synthesis of AgNPs

The synthesis of silver nanoparticles using *C. gigantea* leaf extract (AgNPs-LCg) was carried out by mixing 90 mL AgNO_3 (2, 5, and 9 mM, separately) with 10 mL of *C. gigantea* leaf extract (Figure 8). The reaction was incubated at room temperature ($25 \pm 1^\circ\text{C}$) under constant stirring using a magnetic stirrer at 60 rpm for 48 h in the dark condition [55]. The synthesis of silver nanoparticles using *C. gigantea* flower extract (AgNPs-FCg) was carried out with the same procedure. We then observed the color formed from the reaction. The results of the AgNPs-LCg and AgNPs-FCg reactions were measured for absorbance using UV-Vis spectrophotometry (Shimadzu, UV 2500, Shimadzu Suzhou Instruments Mfg. Co., Ltd., Jiangsu, China) at a wavelength of 300–600 nm and centrifuged (Nuve, NF 800R model, Ankara, Turkey) at $13,000 \times g$ for 10 min.

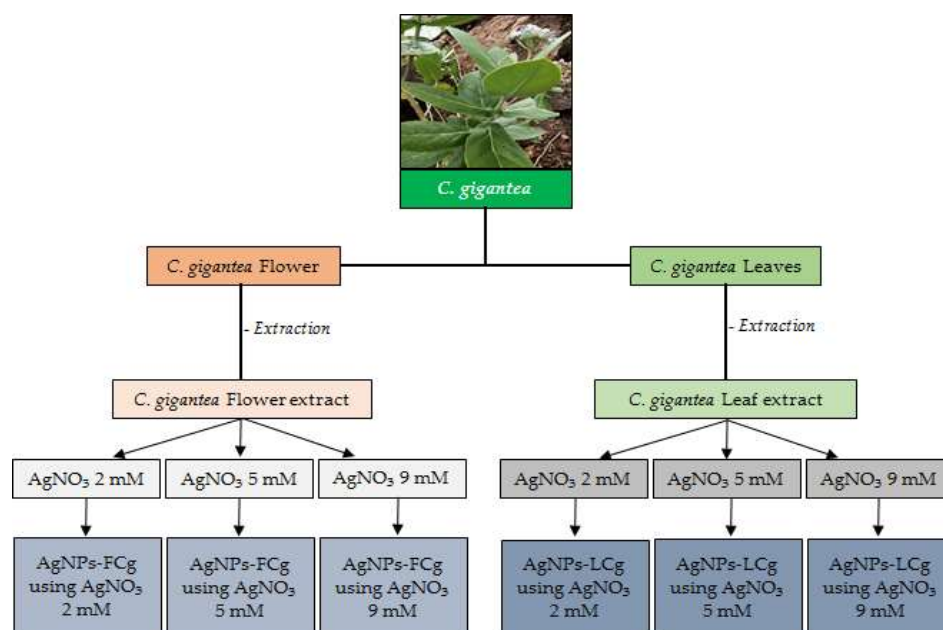


Figure 8. Schematic diagram of the green synthesis of AgNPs-LCg and AgNPs-FCg.

3.5. Characterization of Silver Nanoparticles (AgNPs-LCg and AgNPs-FCg)

AgNPs-LCg and AgNPs-FCg were characterized using Fourier transform infrared (FTIR) spectroscopy (Search 630 FTIR Spectrometer, Agilent Technologies, Santa Clara, CA, USA), and scanning electron microscopy energy-dispersive x-ray spectroscopy (SEM-EDX, Carl Zeiss-Bruker EVO MA 10, Carl Zeiss Microscopy, White Plains, NY, USA). The characterization of the zeta potential value (mV) and polydispersity index (PI) of samples were analyzed using a Zetasizer Nano (Horiba SZ-100, Horiba Mfg. Co., Ltd., Kyoto, Japan).

3.6. Antimicrobial Activity Assay

Antibacterial and antifungal tests were performed using the Kirby-Bauer disc diffusion method. The AgNPs-LCg and AgNPs-FCg were tested for their inhibition zones on colonies of pathogenic bacteria *S. aureus* and *E. coli*, and the fungus *C. albicans*. Both the bacterial colonies were grown in an MHA medium for 24 h at 37 °C. Furthermore, the colonies from the liquid medium were spread on a Petri dish containing MHA agar using a spreader. Prepared sterile paper discs (6 mm in size) were placed on the Petri dishes used for inoculation. AgNPs-LCg and AgNPs-FCg samples with various concentrations (2, 5, or 9 mM) were then loaded onto each paper disc. The positive control used for the Gram-positive antibacterial assay was vancomycin, while the positive control for the Gram-negative antibacterial assay was gentamicin. The inhibitory diameter was measured after incubation at 24 h (37 °C). The antifungal activity of *C. albicans* was also carried out with the same method but the medium used was SDA media, and the positive control used for the antifungal assay was ketoconazole. The assays were prepared in triplicate.

4. Conclusions

We successfully carried out green synthesis of AgNPs using leaf and flower extracts of *Calotropis gigantea*, which grows in the geothermal manifestation Ie Seu-Um, Aceh Besar, Indonesia. Using AgNO₃ as a metal precursor with concentrations of 2, 5, and 9 mM, it is known to form SPR peaks in the 410–460 nm range. The FTIR results also showed the functional groups detected in AgNPs-FCg and AgNPs-LCg. In addition, AgNPs-FCg and AgNPs-LCg have a sphere-shaped morphology, good stability, and antimicrobial activity against Gram-positive bacteria, Gram-negative bacteria, and fungi. AgNPs-FCg is known to have a larger inhibition zone than AgNPs-LCg. As a result of the findings regarding nanoparticle size, we recommend additional research into reaction process optimization to reduce the generally accepted nanoparticle size to values lower than those found in this study.

Author Contributions: Conceptualization, R.I., K.K. and P.K.; methodology, P.K., R.I. and K.K.; software, P.K. and M.I.; project administration, Z.J., G.M.I., R.N. and M.R.; investigation, P.K., R.I. and K.K.; data curation, Z.J., G.M.I., Z.H., E.S., T.E.T. and R.N.; writing—original draft preparation, P.K., R.I. and K.K.; writing—review and editing, P.K., R.I., K.K., M.I. and E.S.; visualization, K.K. and P.K.; supervision, R.I.; funding acquisition, R.I. All authors have read and agreed to the published version of the manuscript.

Funding: This research was funded by Universitas Syiah Kuala, Kementerian Pendidikan, Kebudayaan, Riset dan Teknologi Indonesia through “Program Riset Unggulan USK Percepatan Doktor” grant number 487/UN11/SPK/PNBP/2022.

Institutional Review Board Statement: Not applicable.

Informed Consent Statement: Not applicable.

Data Availability Statement: Data that support the findings of this study are available from the corresponding author upon reasonable request.

Acknowledgments: We thank Universitas Syiah Kuala and the LPPM at Universitas Syiah Kuala for their help and support.

Conflicts of Interest: The authors declare no conflict of interest.

Sample Availability: Samples of the compounds are available from the authors.

References

1. Tallei, T.E.; Yelnetty, A.; Marfuah, S. Evaluation of the Potential for Immunomodulatory and Anti-Inflammatory Properties of Phytoconstituents Derived from Pineapple [*Ananas comosus* (L.) Merr.] Peel Extract Using an In Silico Approach. *Philipp. J. Sci.* **2022**, *151*, 397–410.
2. Khairan, K.; Astuti, Y.; First, I.S. Gel Formulation of Ethyl Acetate Garlic Extraction and Its Activity Against Staphylococcus Epidermis. *J. Chem. Nat. Resour.* **2019**, *1*, 69–78. [[CrossRef](#)]
3. Khairan, K.; Septiya, S. Murniana Antibacterial Activity of Magnolia Alba Flower Extracts on Staphylococcus Epidermidis and Staphylococcus Aureus. In *IOP Conference Series: Earth and Environmental Science, Proceedings of the 10th Annual International Conference (AIC) on Environmental and Life Sciences (ELS), Banda Aceh, Indonesia, 15–16 October 2020*; IOP Publishing: Bristol, UK, 2021; Volume 711, p. 711. [[CrossRef](#)]
4. Seriana, I.; Akmal, M.; Darusman; Wahyuni, S.; Khairan, K. Sugito Phytochemicals Characterizations of Neem (*Azadirachta indica* A. Juss) Leaves Ethanolic Extract: An Important Medicinal Plant as Male Contraceptive Candidate. *Rasayan J. Chem.* **2021**, *14*, 343–350. [[CrossRef](#)]
5. Khairan, K.; Aulina, A.; Yusra, N.; Eriana, C.N.; Bahi, M.; Syaukani, S.; Sriwati, R.; Jacob, C. Termiticidal and Nematicidal Activities of Five Extracts from Garlic (*Allium sativum*). In *Journal of Physics: Conference Series, Volume 1882, The 1st South East Asia Science, Technology, Engineering and Mathematics International Conference (SEA-STEM IC) 2020, Banda Aceh, Indonesia, 20–22 October 2020*; IOP Publishing: Bristol, UK, 2021; Volume 1882. [[CrossRef](#)]
6. Mousavi, S.S.; Karami, A.; Haghighi, T.M.; Tumilaar, S.G.; Fatimawali; Idroes, R.; Mahmud, S.; Celik, I.; Ağagündüz, D.; Tallei, T.E.; et al. In Silico Evaluation of Iranian Medicinal Plant Phytoconstituents as Inhibitors against Main Protease and the Receptor-Binding Domain of Sars-Cov-2. *Molecules* **2021**, *26*, 5724. [[CrossRef](#)]
7. Khairan, K.; Idroes, R.; Tumilaar, S.G.; Tallei, T.E.; Idroes, G.M.; Rahmadhany, F.; Futri, M.U.; Dinura, N.M.; Mauliza, S.; Diana, M.; et al. Molecular Docking Study of Fatty Acids from Pliek U Oil in the Inhibition of SARS-CoV-2 Protein and Enzymes. In *IOP Conference Series: Materials Science and Engineering, The 10th Annual International Conference on Science and Engineering (10th AIC 2020), Banda Aceh, Indonesia, 15–16 October 2020*; IOP Publishing: Bristol, UK, 2021; Volume 1087. [[CrossRef](#)]
8. Tallei, T.E.; Tumilaar, S.G.; Niode, N.J.; Fatimawali, F.; Kepel, B.J.; Idroes, R.; Effendi, Y. Potential of Plant Bioactive Compounds as SARS-CoV-2 Main Protease (Mpro) and Spike (S) Glycoprotein Inhibitors: A Molecular Docking Study. *Scientifica* **2020**, *2020*, 6307457. [[CrossRef](#)]
9. Dutta, M.; Nezam, M.; Chowdhury, S.; Rakib, A.; Paul, A.; Sami, S.A.; Uddin, M.Z.; Rana, M.S.; Hossain, S.; Effendi, Y.; et al. Appraisals of the Bangladeshi Medicinal Plant Calotropis Gigantea Used by Folk Medicine Practitioners in the Management of COVID-19: A Biochemical and Computational Approach. *Front. Mol. Biosci.* **2021**, *8*, 625391. [[CrossRef](#)]
10. Abubakar, A.; Yusuf, H.; Syukri, M.; Nasution, R.; Karma, T.; Munawar, A.A.; Idroes, R. Chemometric Classification of Geothermal and Non-Geothermal Ethanol Leaf Extract of Seurapoh (*Chromolaena odorata* Linn) Using Infrared Spectroscopy. *Earth Environ. Sci.* **2021**, *667*, 012070. [[CrossRef](#)]
11. Nuraskin, C.; Marlina; Idroes, R.; Soraya, C. Djufri Identification of Secondary Metabolite of Laban Leaf Extract (*Vitex pinnata* L) from Geothermal Areas and Non-Geothermal of Agam Mountains in Aceh Besar, Aceh Province, Indonesia. *Rasayan, J. Chem.* **2020**, *13*, 18–23. [[CrossRef](#)]
12. Idroes, R.; Yusuf, M.; Saiful, S.; Alatas, M.; Subhan, S.; Lala, A.; Muslem, M.; Suhendra, R.; Idroes, G.M.; Marwan, M.; et al. Geochemistry Exploration and Geothermometry Application in the North Zone of Seulawah Agam, Aceh Besar District, Indonesia. *Energies* **2019**, *12*, 4442. [[CrossRef](#)]
13. Idroes, R.; Marwan, M.; Yusuf, M.; Muslem, M.; Helwani, Z. Geochemical Investigation on Jaboi Manifestation, Jaboi Volcano, Sabang, Indonesia. *Int. J. Geomate* **2021**, *20*, 170–185. [[CrossRef](#)]
14. Marwan, M.; Yanis, M.; Nugraha, G.S.; Zainal, M.; Arahman, N.; Idroes, R.; Dharna, D.B.; Saputra, D.; Gunawan, P. Mapping of Fault and Hydrothermal System beneath the Seulawah Volcano Inferred from a Magnetotellurics Structure. *Energies* **2021**, *14*, 6091. [[CrossRef](#)]
15. Idroes, R.; Yusuf, M.; Alatas, M.; Subhan; Lala, A.; Muslem; Suhendra, R.; Idroes, G.M.; Suhendrayatna; Marwan; et al. Geochemistry of Warm Springs in the Ie Brôuk Hydrothermal Areas at Aceh Besar District. In *IOP Conference Series: Materials Science and Engineering, The 8th Annual International Conference (AIC) 2018 on Science and Engineering, Banda Aceh, Indonesia, 12–14 September 2018*; IOP Publishing: Bristol, UK, 2019; Volume 523. [[CrossRef](#)]
16. Idroes, R.; Yusuf, M.; Alatas, M.; Subhan, S.; Lala, A.; Saiful, S.; Suhendra, R.; Idroes, G.M.; Marwan, M. Geochemistry of Hot Springs in the Ie Seu'um Hydrothermal Areas at Aceh Besar District, Indonesia. In *IOP Conference Series: Materials Science and Engineering, The 3rd International Conference on Chemical Engineering Sciences and Applications 2017 (3rd ICChESA 2017), Banda Aceh, Indonesia, 20–21 September 2017*; IOP Publishing: Bristol, UK, 2018; Volume 334. [[CrossRef](#)]
17. Idroes, R.; Yusuf, M.; Alatas, M.; Subhan; Lala, A.; Muhammad; Suhendra, R.; Idroes, G.M.; Marwan. Geochemistry of Sulphate Spring in The Ie Jue Geothermal Areas at Aceh Besar District, Indonesia. In *IOP Conference Series: Materials Science and Engineering*,

- The 8th Annual International Conference (AIC) 2018 on Science and Engineering, Banda Aceh, Indonesia, 12–14 September 2018*; IOP Publishing: Bristol, UK, 2019; Volume 523.
18. Ningsih, D.S.; Idroes, R. In Vitro Cytotoxicity of Ethanolic Extract of The Leaf of *Calotropis Gigantea* from Ie Jue Geothermal Area, Aceh-Indonesia, And Its Mouthwash Formulation Against Dental Pulp Cells. *J. Applied Pharm. Sci.* **2022**, *12*, 133–143. [[CrossRef](#)]
 19. Idroes, G.M.; Tallei, T.E.; Idroes, R.; Muslem; Riza, M.; Suhendrayatna. The Study of *Calotropis Gigantea* Leaf Metabolites from Ie Brouk Geothermal Area Lamteuba-Aceh Besar Using Molecular Docking. In *IOP Conference Series: Earth and Environmental Science, The 2nd International Conference on Agriculture and Bio-industry, Banda Aceh, Indonesia, 27–28 October 2020*; IOP Publishing: Bristol, UK, 2021; Volume 667. [[CrossRef](#)]
 20. Idroes, R.; Khairan, K.; Fakri, F.; Zulfendi, Z. *Skrining Aktifitas Tumbuhan Yang Berpotensi Sebagai Bahan Antimikroba Di Kawasan Ie Seu Um Aceh Besar*; Syiah Kuala Universiti Press: Banda Aceh, Indonesia, 2016; ISBN 978-602-1270-52-3.
 21. Bruna, T.; Maldonado-Bravo, F.; Jara, P.; Caro, N. Silver Nanoparticles and Their Antibacterial Applications. *Int. J. Mol. Sci.* **2021**, *22*, 7202. [[CrossRef](#)] [[PubMed](#)]
 22. Agnihotri, S.; Mukherji, S.; Mukherji, S. Immobilized Silver Nanoparticles Enhance Contact Killing and Show Highest Efficacy: Elucidation of The Mechanism of Bactericidal Action of Silver. *Nanoscale* **2013**, *5*, 7328–7340. [[CrossRef](#)]
 23. Quinteros, M.A.; Cano Aristizábal, V.; Dalmasso, P.R.; Paraje, M.G.; Páez, P.L. Oxidative Stress Generation of Silver Nanoparticles in Three Bacterial Genera and Its Relationship with The Antimicrobial Activity. *Toxicol. Vitro* **2016**, *36*, 216–223. [[CrossRef](#)]
 24. Goma, E.Z. Silver Nanoparticles as an Antimicrobial Agent: A Case Study on *Staphylococcus Aureus* and *Escherichia Coli* as Models for Gram-Positive and Gram-Negative Bacteria. *J. Gen. Appl. Microbiol.* **2017**, *63*, 36–43. [[CrossRef](#)] [[PubMed](#)]
 25. Silva, M.C.; Werlang, H.M.; Vandresen, D.; Fortes, P.C.; Pascotto, C.R.; Lucio, L.C.; Ferreto, L.E. Genetic, Antimicrobial Resistance Profile and Mortality Rates of *Acinetobacter Baumannii* Infection in Brazil: A Systematic Review. *Narra J.* **2022**, *2*, e68. [[CrossRef](#)]
 26. Harahap, D.; Niaci, S.; Mardina, V.; Zaura, B.; Qanita, I.; Purnama, A.; Pispita, K.; Rizki, D.R.; Iqhrammullah, M. Antibacterial Activities of Seven Ethnomedicinal Plants from Family Annonaceae. *J. Adv. Pharm. Technol. Res.* **2022**, *13*, 148–153. [[CrossRef](#)]
 27. Salayov, A.; Bedlovičová, Z. Green Synthesis of Silver Nanoparticles with Antibacterial Activity Using Various Medicinal Plant Extracts: Morphology and Antibacterial Efficacy. *Nanomaterials* **2021**, *11*, 1005. [[CrossRef](#)]
 28. Jain, A.S.; Pawar, P.S.; Sarkar, A.; Junnuthula, V.; Dyawanapelly, S. Bionanofactories for Green Synthesis of Silver Nanoparticles: Toward Antimicrobial Applications. *Int. J. Mol. Sci.* **2021**, *22*, 11993. [[CrossRef](#)]
 29. Sharma, V.; Kaushik, S.; Pandit, P.; Dhull, D.; Yadav, J.P.; Kaushik, S. Green Synthesis of Silver Nanoparticles From Medicinal Plants And Evaluation of Their Antiviral Potential Against Chikungunya Virus. *Appl. Microbiol. Biotechnol.* **2019**, *103*, 881–891. [[CrossRef](#)] [[PubMed](#)]
 30. Anbu, P.; Gopinath, S.C.B.; Shik, H.; Lee, C. Temperature-Dependent Green Biosynthesis and Characterization of Silver Nanoparticles Using Balloon Flower Plants and Their Antibacterial Potential. *J. Mol. Struct.* **2019**, *1177*, 302–309. [[CrossRef](#)]
 31. Tanase, C.; Berta, L.; Coman, A.; Ros, I.; Man, A.; Toma, F.; Mocan, A.; Nicolescu, A.; Jakab-farkas, L. Antibacterial and Antioxidant Potential of Silver Nanoparticles Biosynthesized Using the Spruce Bark Extract. *Nanomaterials* **2019**, *9*, 1541. [[CrossRef](#)] [[PubMed](#)]
 32. Gemishev, O.; Panayotova, M.; Gicheva, G.; Mintcheva, N. Green Synthesis of Stable Spherical Monodisperse Silver Nanoparticle Using a Cell-Free Extract of *Trichoderma Reesei*. *Materials* **2022**, *15*, 481. [[CrossRef](#)]
 33. Al-otibi, F.; Perveen, K.; Al-saif, N.A.; Alharbi, R.I.; Bokhari, N.A.; Albasher, G.; Al-otaibi, R.M.; Al-mosa, M.A. Biosynthesis of Silver Nanoparticles Using *Malva Parviflora* and Their Antifungal Activity. *Saudi J. Biol. Sci.* **2021**, *28*, 2229–2235. [[CrossRef](#)]
 34. Mathew, S.; Victo, C.P.; Sidhi, J.; Thanzeela, B. Biosynthesis of Silver Nanoparticle Using Flowers of *Calotropis gigantea* (L.) W.T. Aiton and Activity Against Pathogenic Bacteria. *Arab. J. Chem.* **2020**, *13*, 9139–9144. [[CrossRef](#)]
 35. Haggag, E.G.; Elshamy, A.M.; Rabeh, M.A.; Gabr, N.M.; Salem, M.; Youssif, K.A.; Samir, A.; Bin Muhsinah, A.; Alsayari, A.; Abdelmohsen, U.R. Antiviral Potential of Green Synthesized Silver Nanoparticles of *Lampranthus Coccineus* And *Malephora Lutea*. *Int. J. Nanomed.* **2019**, *14*, 6217–6229. [[CrossRef](#)]
 36. Rakib-Uz-Zaman, S.M.; Apu, E.H.; Muntasir, M.N.; Mowna, S.A.; Khanom, M.G.; Jahan, S.S.; Akter, N.; Khan, M.A.R.; Shuborna, N.S.; Shams, S.M.; et al. Biosynthesis of Silver Nanoparticles from *Cymbopogon Citratus* Leaf Extract and Evaluation of Their Antimicrobial Properties. *Challenges* **2022**, *13*, 18. [[CrossRef](#)]
 37. Alahmad, A.; Al-zereini, W.A.; Hijazin, T.J.; Al-madanat, O.Y.; Alghoraibi, I.; Al-qaralleh, O.; Al-qaraleh, S.; Feldhoff, A.; Walter, J.; Scheper, T. Green Synthesis of Silver Nanoparticles Using *Hypericum perforatum* L. Aqueous Extract with the Evaluation of Its Antibacterial Activity against Clinical and Food Pathogens. *Pharmaceutics* **2022**, *14*, 1104. [[CrossRef](#)]
 38. Govindan, L.; Anbazhagan, S.; Altemimi, A.B.; Lakshminarayanan, K.; Kuppan, S.; Pratap-Singh, A.; Kandasamy, M. Efficacy of Antimicrobial and Larvicidal Activities of Green Synthesized Silver Nanoparticle Using Leaf Extract of *Plumbago Auriculata* Lam. *Plants* **2020**, *9*, 1577. [[CrossRef](#)]
 39. Pryshchepa, O.; Pomastowski, P.; Buszewski, B. Silver Nanoparticles: Synthesis, Investigation Techniques, and Properties. *Adv. Colloid Interface Sci.* **2020**, *284*, 87–100. [[CrossRef](#)] [[PubMed](#)]
 40. Ali, E.M.; Abdallah, B.M. Effective Inhibition of Candidiasis Using an Eco-Friendly Leaf Extract of *Calotropis-Gigantea*-Mediated Silver Nanoparticles. *Nanomaterials* **2020**, *10*, 422. [[CrossRef](#)] [[PubMed](#)]
 41. Ali, D.M.; Sasikala, M.; Gunasekaran, M.; Thajuddin, N. Biosynthesis and Characterization of Silver Nanoparticles Using Marine Cyanobacterium, *Oscillatoria Willei* NTDM01. *J. Nanomater. Biostruct.* **2011**, *6*, 385–390.
 42. Mirda, E.; Idroes, R.; Khairan, K.; Tallei, T.E.; Ramli, M.; Earlia, N.; Maulana, A.; Idroes, G.M.; Muslem, M.; Jalil, Z. Synthesis of Chitosan-Silver Nanoparticle Composite Spheres and Their Antimicrobial Activities. *Polymers* **2021**, *13*, 3990. [[CrossRef](#)]

43. Almatroudi, A.; Khadri, H.; Azam, M.; Rahmani, A.H.; Khaleefah, F.; Khaleefah, A.; Khateef, R.; Ansari, M.A.; Allemailem, K.S. Antibacterial, Antibiofilm and Anticancer Activity of Biologically Synthesized Silver Nanoparticles Using Seed Extract of *Nigella Sativa*. *Processes* **2020**, *8*, 388. [[CrossRef](#)]
44. Kambale, E.K.; Nkanga, C.I.; Mutonkole, B.P.I.; Bapolisi, A.M.; Tassa, D.O.; Liesse, J.M.I.; Krause, R.W.M.; Memvanga, P.B. Green Synthesis of Antimicrobial Silver Nanoparticles Using Aqueous Leaf Extracts from Three Congolese Plant Species (*Brillantaisia patula*, *Crossopteryx febrifuga* and *Senna siamea*). *Heliyon* **2020**, *6*, e04493. [[CrossRef](#)]
45. Alsalhi, M.S.; Elangovan, K.; Jacob, A.; Ranjitsingh, A.; Murali, P.; Devanesan, S. Synthesis of Silver Nanoparticles Using Plant Derived 4-N-Methyl Benzoic Acid And Evaluation of Antimicrobial, Antioxidant And Antitumor Activity. *Saudi J. Biol. Sci.* **2019**, *26*, 970–978. [[CrossRef](#)]
46. Kokila, T.; Ramesh, P.S.; Geetha, D. Biosynthesis of AgNPs Using Carica Papaya Peel Extract and Evaluation of Its Antioxidant and Antimicrobial Activities. *Ecotoxicol. Environ. Saf.* **2016**, *134*, 467–473. [[CrossRef](#)]
47. Venkatachalam, S. *Chapter 6. Ultraviolet and Visible Spectroscopy Studies of Nanofillers and Their Polymer Nanocomposites*; Elsevier Inc.: Amsterdam, The Netherlands, 2016; ISBN 9780323401838.
48. Jaswal, T.; Gupta, J. A Review on the Toxicity of Silver Nanoparticles on Human Health. *Mater. Today Proc.* **2021**, 1–5. [[CrossRef](#)]
49. Al-otibi, F.; Al-ahaidib, R.A.; Alharbi, R.I.; Al-otaibi, R.M.; Albasher, G. Antimicrobial Potential of Biosynthesized Silver Nanoparticles by *Aaronsohnia Factorovskiyi* Extract. *Molecules* **2021**, *26*, 130. [[CrossRef](#)]
50. Pietta, P.G. Flavonoids as Antioxidants. *J. Nat. Prod.* **2000**, *63*, 1035–1042. [[CrossRef](#)] [[PubMed](#)]
51. Van Acker, S.A.B.E.; Van Den Berg, D.J.; Tromp, M.N.J.L.; Griffioen, D.H.; Van Bennekom, W.P.; Van Der Vijgh, W.J.F.; Bast, A. Structural Aspects of Antioxidant Activity of Flavonoids. *Free Radic. Biol. Med.* **1996**, *20*, 331–342. [[CrossRef](#)]
52. Nayem, S.M.A.; Sultana, N.; Haque, A.; Miah, B.; Hasan, M.; Islam, T.; Mahedi, H.; Awal, A.; Uddin, J.; Aziz, A.; et al. Green Synthesis of Gold and Silver Nanoparticles by Using *Amorphophallus paeoniifolius* Tuber Extract and Evaluation of Their Antibacterial Activity. *Molecules* **2020**, *25*, 4773. [[CrossRef](#)] [[PubMed](#)]
53. Chouhan, S.; Guleria, S. Green Synthesis of AgNPs Using Cannabis Sativa Leaf Extract: Characterization, Antibacterial, Anti-Yeast and Alpha-Amylase Inhibitory Activity. *Mater. Sci. Energy Technol.* **2020**, *3*, 536–544. [[CrossRef](#)]
54. Musman, M. *Kimia Bahan Alam Laut*; Syiah Kuala University Press: Banda Aceh, Indonesia, 2013; ISBN 9789798278938.
55. Sorubavalli, U.; Vadivazhagi, M.K.; Vadivelu, J. Antioxidant and Antimicrobial Activity of Calotrophis Mediated Silver Nanoparticles. *J. Compos. Theory* **2019**, *XII*, 303–312.